© 2023 The Author(s). Published by Elsevier B.V. This is an open access article under the Creative Commons Attribution-NonCommercial-NoDerivatives 4.0 International (CC BY-NC-ND 4.0) License.

The following article appeared in Carbon Trends, Volume 10, March 2023, 100235 and may be found at: https://doi.org/10.1016/j.cartre.2022.100235

Carbon Trends 10 (2023) 100235

Contents lists available at ScienceDirect

Carbon Trends

journal homepage: www.elsevier.com/locate/cartre

Metal decorated carbon nanotube aerogels from sodium polyacrylate crosslinking by divalent ions

Andres Fest[a,b], Ferdinando Tristán[a], Wendi Perez-Vigueras[a], Gladis Judith Labrada-Delgado[c], David Meneses-Rodríguez[d], Sofía Magdalena Vega-Díaz[a,*]

[a] Departamento de Ingeniería Química, Tecnológico Nacional de México/Instituto Tecnológico de Celaya, Avenida Tecnológico esq., A. García Cubas #600 Pt, Celaya, Guanajuato CP 38010, Mexico
[b] Department of Materials Science and Engineering, The Pennsylvania State University, University Park, PA 16802, USA.
[c] LINAN-IPICYT, Camino a la Presa San José 2055. Col. Lomas 4 sección, San Luis Potosí S.L.P. CP 78216, Mexico
[d] Cátedras-CONACYT CINVESTAV, Mérida Km 6, Carretera Antigua a Progreso, Cordemex, Mérida, Yucatán CP 97310, Mexico

ARTICLE INFO

Keywords:
Aerogel
Carbon nanotubes
Ionic interactions

ABSTRACT

In this work sodium polyacrylate functionalized carbon nanotube aerogels were prepared from aqueous medium by simple ionic cross-linking using copper nitrate and calcium chloride as cation sources to obtain self-standing 3D structure. The complete procedure involves gelation of functionalized carbon nanotubes, freeze-drying and calcination to obtain the self-standing structures. These structures were characterized by scanning electron microscopy (SEM), Raman spectroscopy, X-ray photoelectron spectroscopy (XPS) and X-ray diffraction (XRD). The self-standing structure is formed by entangled carbon nanotubes arranged in sheet-like assemblies. After calcination, the presence of the carboxylate contribution in C1s XPS spectra in the cross-linked materials, suggests its important role in thermal stability of the aerogels. This method also allowed obtaining metal particles embedded within the carbon nanotube network of the final material, which is a feature that could also contribute to the overall properties of the aerogel.

1. Introduction

Since their discovery, the properties of carbon nanotubes have granted them great attention for applications as diverse as polymer and metal reinforcing, solar cells, displaying, electromagnetic shielding, catalysis, batteries, and other energy related applications. In all cases, the goal is to develop materials that allow taking full advantage of their properties at the macroscopic scale. One of the commonly used procedures to accomplish this is through the preparation of free-standing 3D materials.

As free-standing materials, carbon nanotubes have been prepared in the form of fibers, mats, films, forests, foams, sheets, aerogels, and sponges. Low density highly porous 3D networks have been of interest for several years, an interest that is reflected in the diversity of methods reported for CNT aerogel preparation, with methods like single and multiple step CVD [1], chemical cross-link [2,3], polymer reinforcement [4–6] and freeze-casting [7] being amongst the most commonly used. All these methods have in common the attempt to increase the stiffness of the aerogel while using low amounts of binders, if any, to prevent a possible negative effect on the final material properties.

Sodium polyacrylate is a polyelectrolyte, usually used as an absorbent agent due to its high affinity to water. When exposed to polyvalent cations in liquid solution, a process of ionic exchange is favored, resulting in the formation of a gel due to crosslinks between polyacrylate chains. This phenomenon has been known for a long time [8] and used in applications like the formation of templates [9].

The functionalization and grafting of carbon nanotubes with sodium polyacrylate and its acid form, polyacrylic acid, have been found to improve their poor dispersibility in water [10–12]. More recently, porous materials have been prepared by crosslinking sodium polyacrylate with divalent cations, with emphasis in the obtention of both amorphous carbon structures [13] and metallic frameworks [14,15]. In both cases, polyacrylate gels are reported to provide steric hinderance, prevent agglomeration and serve as a template that influences the final microstructure and the morphology of the prepared materials [15].

There are some reports of nanostructured aerogels prepared using polyacrylic acid as reinforcement [16,17], crosslinked by a mechanism that takes advantage of the thermal reduction of the carboxylic groups, however, to the best of our knowledge there is still no report on the use of the gelation of sodium polyacrylate with divalent ions to generate carbon nanotube nanostructured aerogels via freeze-casting.

* Corresponding author.
E-mail address: sofia.vega@iqcelaya.itc.mx (S.M. Vega-Díaz).

https://doi.org/10.1016/j.cartre.2022.100235
Received 27 September 2022; Received in revised form 28 November 2022; Accepted 29 November 2022
2667-0569/© 2022 The Authors. Published by Elsevier Ltd. This is an open access article under the CC BY-NC-ND license (http://creativecommons.org/licenses/by-nc-nd/4.0/)

In the present work, carbon nanotube aerogels are prepared by a simple yet effective freeze-casting method, where ionic exchange is used as intermediary step to from gels of sodium polyacrylate functionalized carbon nanotubes. In principle the preparation of aerogels using this technique can be done using any divalent cation, with the advantage of generating metal oxide particles homogeneously embedded within the carbon nanotube network of the final material.

2. Experimental details

2.1. Materials and reagents

Nitrogen doped multiwalled carbon nanotubes (CNx) were obtained from a previous synthesis performed following the method reported by Terrones et al. [18]. Sodium polyacrylate 30% wt. solution (Mw ~1200) was bought from Sigma-Aldrich. Copper nitrate was bought from J.T. Baker. Calcium chloride was bought from Jalmek Scientific. Hydrogen peroxide was bought from Fermont. All chemicals were reactive grade and used without further purification.

2.2. Sample preparation

2.2.1. Carbon nanotube purification

In order to reduce the amount of amorphous carbon and other unwanted byproducts, nitrogen doped carbon nanotubes were purified using a modification of the procedure reported by Belmonte et al. [19], as follows: 40 mg of carbon nanotubes (CNx) were added under sonication to a beaker containing 60 ml of hydrogen peroxide and continuously stirred. After one hour, the obtained suspension was filtered, washed with several volumes of deionized water, and dried in air at 60 °C overnight.

2.2.2. Carbon nanotube functionalization

For the functionalization of carbon nanotubes, 10 mg of the purified carbon nanotubes (p-CNx) were dispersed in 20 ml of deionized water in a sonic bath for 1 h, added dropwise to 20 ml of a 4 mg/ml aqueous solution of sodium polyacrylate and then left in the sonic bath for another hour. This suspension was filtered and washed with deionized water to remove unbind polymer residues. The filtration cake was immediately resuspended in water to a final concentration of 0.5 mg/ml. Multiple batches were synthetized following this procedure, stirred together to prepare a stock suspension, and stored for later use.

2.2.3. Preparation of aerogels

To generate the gels, 10 ml of the functionalized carbon nanotube suspension were vigorously stirred with 5 ml of a 0.3 M solution of a divalent cation salt. Additionally, a control aerogel was prepared using deionized water instead of cation solution and given the same exact following treatments.

To remove salt excess from the material, the gels were washed three times by centrifugation at low speeds, replacing the supernatant with deionized water every time. The last wash was followed by a final centrifugation at 2465 RCF for 15 min, to increase the gel density.

In a freeze-casting process, the obtained gel was frozen overnight in a conventional freezer, at a temperature of -15 ± 5 °C, and then lyophilized in a Labconco FreeZone 2.5 freeze dry system until complete absence of ice. Finally, the lyophilized aerogels (AG, AG-Cu & AG-Ca) were calcinated at 450 °C for two hours in a tube furnace under nitrogen flow to obtain the final materials (AG-T, AG-Cu-T, AG-Ca-T).

3. Characterization

The prepared materials were characterized using SEM (JEOL JSM-7600F, using silicon wafers to support pieces of aerogel), as well as FEI DUAL BUEAM HELIOS NANOLAB600 SEM, using ultra high resolution (UHR) reaching 100 000x, Raman spectroscopy (WI Tec Alpha 300, 488 nm laser), XRD (Bruker D-8 Advance diffractometer, Cu-Kα1 radiation,40kv, 30 mA), XPS (Thermo Scientific K-ALPHA Photoelectron Spectrometer, Al-Kα monochromatic X-ray beam, 40 W. Irradiated area: 400 μm^2) and TGA (TA Instruments Discovery, from 30 °C to 900 °C at a rate of 10 °C/min, in air atmosphere). Peak fitting of the obtained XPS spectra was performed using CasaXPS software (V. 2.3.18) assuming Shirley background. Raw Raman spectra were fit by the Levenberg-Marquardt method using 5 bands located at 1624, 1583 1487, 1351 and 1220 cm^{-1}, as reported by Maldonado et al. [20].

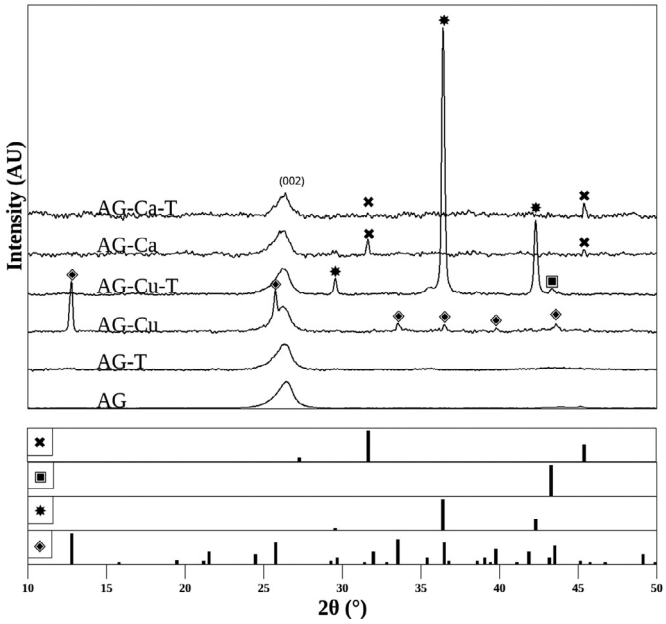

Fig. 1. XRD diffractograms of the prepared aerogels. (▣: Metallic copper; ◈: Rouaite (Cu_2 (NO_3) $(OH)_3$); ✸: Cuprite (Cu_2O); X: Halite (NaCl)). Relative diffraction intensities obtained from PDF cards are included as reference.

4. Results and discussion

This simple freeze-casting method allows to produce the macroscopic self-standing aerogels depicted on the digital pictures available in Fig. S1 of the supporting information.

An initial coarse indication of the compounds present on the prepared aerogels was determined using XRD by comparing the diffractograms of the prepared aerogels and the nanotube powders, shown on Figs. 1 and S2, to powder diffraction files (PDFs) obtained from the ICDD PDF-4+ database [21]. The main diffraction peak in all the samples in the present work is located at circa 26°, which corresponds to the 002 reflection of the multiwalled carbon nanotubes [22]. This is the only peak detected on the control aerogels (AG & AG-T).

The diffractogram of pristine carbon nanotubes, CNx in Fig. S2, shows multiple peaks between 35 and 50° that match the diffraction pattern of cementite, a crystalline phase of iron carbide (Fe_3C) (PDF 00–034–0001 [21]), a byproduct obtained from the iron catalyst used during nanotube synthesis. In the same figure, the diffraction pattern of purified carbon nanotubes (p-CNx) shows the reduction of the intensity of these peaks, due to removal of some of this impurity during the peroxide treatment performed on the ultrasonic bath. The intensity of these carbide peaks is further reduced after the functionalization process (f-CNx).

The diffractogram of the freshly freeze-dried copper treated aerogel (AG-Cu) shows peaks at 12.8, 25.77, 33.5, 36.5, 39.8 and 43.59°, a good match with the reflections of the 001, 002, 120, 121, −202 and 122 crystal planes of rouaite (PDF 00–015–0014 [21]), a metastable polymorph of copper hydroxyl nitrate ($Cu_2(NO_3)(OH)_3$), probably formed

Table 1
D and G band analysis from deconvolution of Raman spectra.

Material	I	D	D"	G	D'	I_D/I_G
CNx	1130.3	1355.6	1476.3	1574.2	1611.5	0.524
p-CNx	1135.4	1356.4	1476.3	1574.1	1609.8	0.516
f-CNx	1177.1	1362.5	1487.0	1578.6	1606.3	0.598
AG	1198.6	1356.5	1494.4	1573.4	1603.8	0.672
AG-T	1146.8	1357.1	1480.5	1575.1	1608.7	0.613
AG-Cu	1113.6	1363.2	1476.4	1580.1	1601.7	0.633
AG-Cu-T	1137.2	1359.3	1484.7	1578.0	1612.6	0.678
AG-Ca	1154.6	1363.7	1504.4	1581.7	1617.1	0.529
AG-Ca-T	1156.5	1363.0	1487.3	1580.5	1615.4	0.515

from residual copper nitrate after lyophilization. After thermal treatment (AG-Cu-T) rouaite peaks disappear, indicating its thermal degradation during the treatment. In the calcined copper treated aerogel, sharp peaks appear at 29.57, 36.42 and 42.31° attributed to the 110, 111 and 200 planes of Cu_2O (PDF 04–007–9767 [21]), respectively, with and additional diffraction peak at 43.3° is attributed to a relatively small amount of metallic copper (PDF 00–004–0836 [21]). By using the most intense cuprite peak (111) and the Scherrer equation, the Cu_2O crystallite size was estimated to be 41.15 nm. It is possible that Cu_2O formation is related to the thermal treatment from the oxidation of metallic Cu as observed in the Fig. 1 diffractogram.

The diffractograms of the calcium chloride treated aerogels (AG-Ca & AG-Ca-T) show peaks at circa 31.6 and 45°, which match the reflections of the 200 and 220 planes of halite (PDF 00–005–0628 [21]) formed as a byproduct of the ion exchange between sodium polyacrylate and calcium chloride. No other crystalline phases could be identified, which suggests that the copper and calcium polyacrylates present on the aerogels are in an amorphous state.

Raman spectroscopy is a useful tool to gain information on the electronic properties of carbon nanotubes. In this study, the 488 nm laser was used because it is more sensitive to the σ (sp^3) bond, which allows a finer analysis of the defects generated by the functionalization of the nanotubes [23–27]. The region surrounding the expected positions of D and G band in the Raman spectra of the prepared aerogels and their starting materials was fit by the Levenberg-Marquardt method using 5 bands located at 1624, 1583 1487, 1351 and 1220 cm^{-1}, corresponding to the D', G, D", D, G and I bands, respectively [20]. Fitted spectra is available in Figs. S4 and S5 on the supporting material. Table 1 summarizes the obtained information.

As can be seen in Table 1, there are not significant differences between the positions of the D and G bands on pristine (CNx) and peroxide purified (P-CNx) carbon nanotubes. Only a slight decrease in the I_D/I_G ratio is observed, which could be attributed to the removal of amorphous carbon from the nanotubes surface. Functionalization with sodium polyacrylate (f-CNx) increased the I_D/I_G ratio beyond its original value, which could be attributed to the addition of sp^3 carbon from the polymer. The displacement observed on the positions of D and G bands and the increase in the width of the G band (Figure S4) can be attributed to interactions with polymer. Liu et al. [11] report blueshifts of about 3 cm^{-1} in D and G bands after functionalization with polyacrylic acid. The greater shift in the present system could be attributed to a more intense interaction between the carbon nanotubes and the polymer due to nitrogen doping within the nanotube.

In the control aerogel (AG), both D and G bands shift closer to their original positions. Probably due to the partial removal of sodium polyacrylate during the gel washing procedure. In contrast, copper nitrate and calcium chloride treated aerogels (AG-Cu and AG-Ca, respectively) preserve D and G band positions like those of the functionalized carbon nanotubes (f-CNx). Ionic exchange generates calcium and copper polyacrylates that are not water-soluble and are not removed during the gel washing procedure. The shifts observed from f-CNx sample to both materials after ionic exchange with Ca (Ag-Ca) and Cu (Ag-Cu) could be related to the ionic interactions between the polymer and the ions.

On the calcinated copper treated aerogel (AG-Cu-T) small displacements of D and G band to lower wavenumbers are attributed to a change of the way that the polymer interacts, probably because of the degradation of copper polyacrylate at this temperatures and the formation of metallic particles [28].

It can also be noticed that while the rest of materials show reduction on their I_D/I_G ratios after thermal treatment, because of the degradation of unlinked polymer, the I_D/I_G ratio on the copper treated aerogel increases after calcination. This is attributed to the formation and attachment of copper oxide particles to the nanotube surface [29].

Raman spectra of calcium treated aerogels (AG-Ca & AG-Ca-T) show no significant change in the positions of D and G bands.

The presence of a shoulder is observed on G band of all materials after functionalization, and especially after thermal treatments. Deconvolution in this zone (Figs. S4 and S5) allows to identify the shoulder as the D' band, related with the turbostratic character in graphene plane stacking [20]. While its intensity and position present only slight variations, it is more perceptible on the calcinated materials because of a reduction on the width of the G band, product of polymer degradation.

For a more detailed characterization on the chemical state on the materials, XPS was performed. Deconvolution of C1s XPS spectra of pristine carbon nanotubes (Fig. S6) showed bands at 284.6 eV, 285.15 eV, 285.94 eV and 286.81 eV attributed to C=C, C–C, C–N and C–O species, respectively [30,31].

After peroxide purification treatment there is an increase in the C-C/C=C area ratio, attributable to the increase of sp^3 carbon species, due to slight oxidation at the nanotube surface by the hydrogen peroxide. This is consistent with the appearance of a new contribution at around 288 eV, attributed to carboxylate groups (O=C-O) [30]. Functionalization with sodium polyacrylate further increased the intensity of this band due to the addition of carboxylate groups present in sodium polyacrylate.

While the carboxylate contribution, at 288 eV, is present on the C1s spectrum of the control aerogel (Fig. 2a), it disappears after the thermal treatment (Fig. 2d), most likely due to thermal reduction. In contrast, copper and calcium treated aerogels preserved this contribution. This showed the improvements in thermal stability of the material, product of ionic crosslinking, since these are the groups involved in the reticulation of the material. The slight decrease in the relative intensity of this signal is attributed to the degradation of unlinked carboxylate groups.

A larger C-C/C=C ratio in can be observed in calcium treated aerogel (AG-Ca), probably because of a more effective retention of polymer after ionic crosslinking. No significant changes are observed after thermal treatment (AG-Ca-T), probably because the degradation temperature of this particular calcium polyacrylate, usually ranging from 470 to 495 °C [32], was likely not exceeded during this treatment.

The obtained O1s spectra (Fig. S6) are composed by three contributions. The first, around 529 eV, is attributed to the presence of iron oxide (529.5 eV) [33], another impurity generated form the iron catalyst used during CNx synthesis. The second contribution, around 531.7 eV, is attributed to the presence of C=O bonds[30], meanwhile the third contribution, around 533.3 eV, is attributed to C–O species[30].

After the nanotube purification treatment, (Fig. S6), the signal attributed to iron oxides reduces its intensity considerably, due to the removal of these impurities. Additionally, there is an increase in the areas of the contributions of C-O and C=O species, due to oxidation on the surface of the nanotubes. Upon functionalization (Fig. S6), the intensity of iron oxides keeps diminishing probably because of the additional sonication time during the functionalization and a new contribution appears at around 535.5 eV, due to the KL_1L_{23} auger line of sodium [34], from the sodium polyacrylate.

Fig. 3 shows SEM micrographs of the thermal treated aerogels. Both cation-treated aerogels (AG-Cu-T & AG-Ca-T) and the control aerogel (AG-T) displayed the formation of tridimensional porous structures with

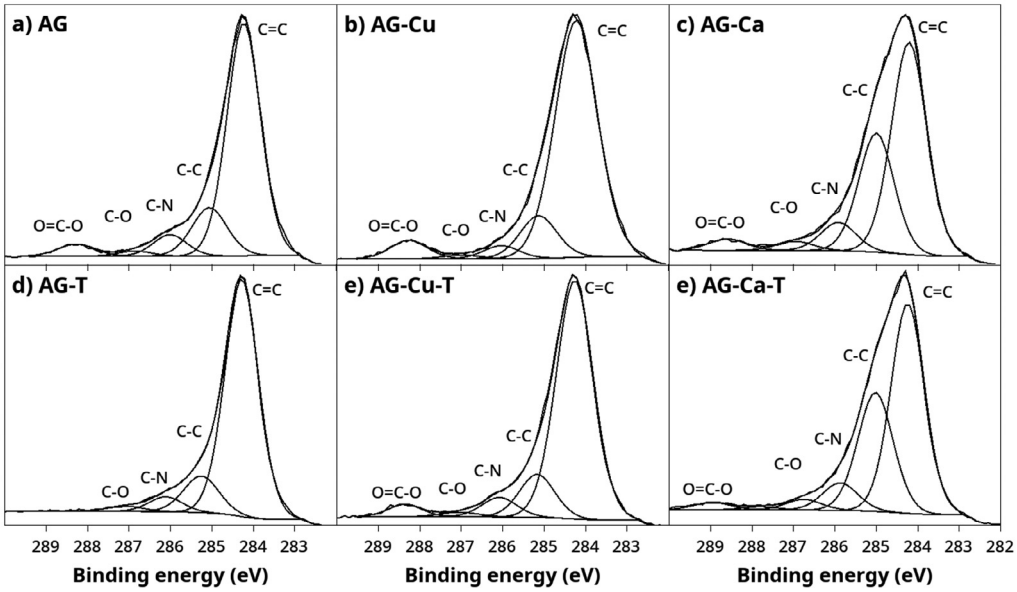

Fig. 2. Deconvoluted high resolution C1s XPS spectra of the prepared aerogels.

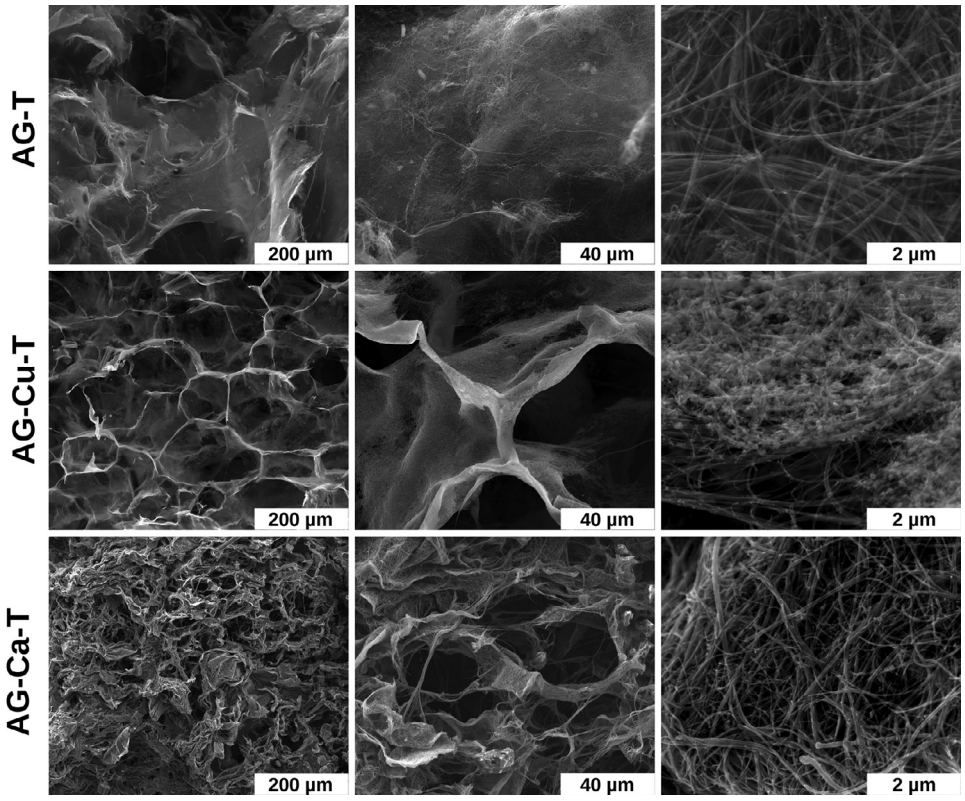

Fig. 3. Secondary electron SEM micrographs of the prepared materials. (200x, 1000x and 20,000x).

walls composed by sheets of entangled carbon nanotubes. This arrangement is a feature frequently seen in the particles that constitute freeze-casted materials [7].

The control aerogel (AG-T) shows a partially collapsed structure with irregular pores, which could be attributed to partial nanotube restacking, due to lack of proper structural support. In addition to the absence of crosslinking cations that bring support, both XPS and Raman spectra suggest that less polymer is retained in this aerogel after the washing step, which probably affects its structural integrity. The copper nitrate treated aerogel (AG-Cu-T) shows a greater number of smaller and more evenly distributed cavities and a greater degree of order is observed.

In the case of calcium treated aerogels (AG-Ca-T) the sheet-like structures form more compact walls with partially collapsed cavities. This apparent collapse should be interpreted as densification due to a larger amount of binder (i.e. polyacrylate) retained by the carbon nanotubes. This hypothesis is supported by the comparatively larger C-C/C=C area ratio present in AG-Ca-T, an indication of a larger amount of non-graphitic carbon in the samples.

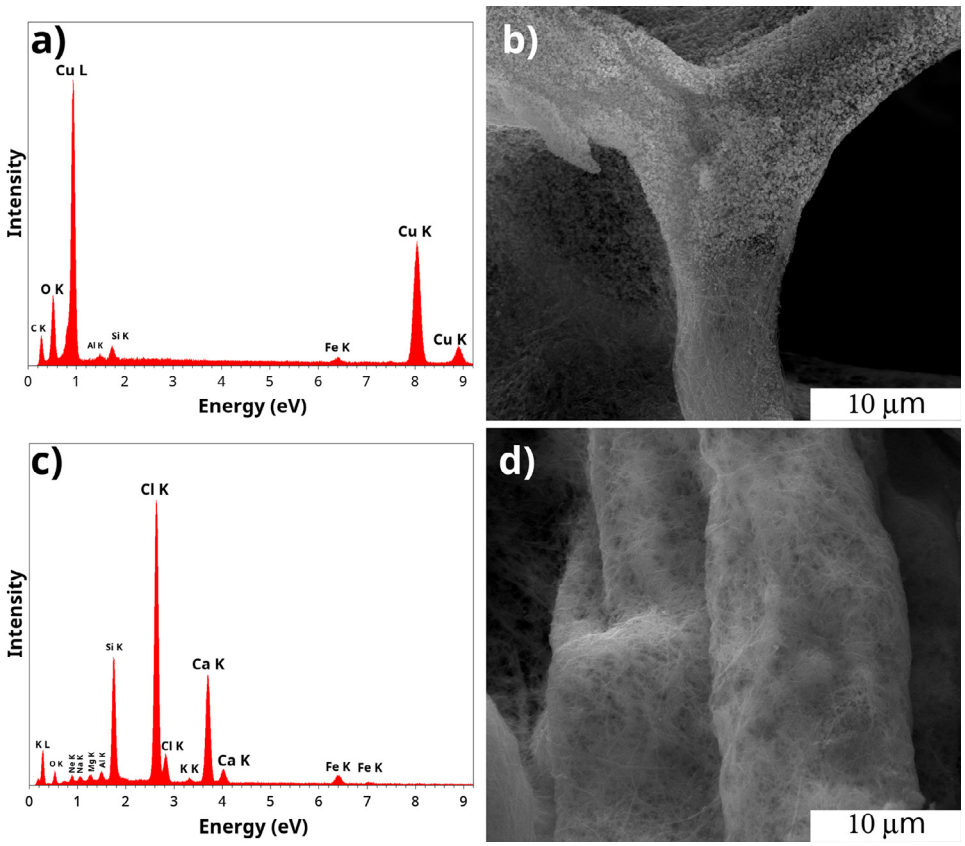

Fig. 4. SEM micrographs of AG-Cu-T and AG-Ca-T aerogels (b & d, respectively) and their corresponding EDX spectra.

In aqueous solution copper nitrate and calcium chloride generate solutions with different pH, being the product of a strong acid and a weak base, copper nitrate tends to acidify aqueous media. On the other hand, calcium chloride generates solutions which pH does not deviate significantly from the neutrality.

The pH has been reported to influence the morphology of structures formed by carbon nanotubes functionalized with polyacrylic acid and its sodium salt. At high pH polyacrylate is tied more strongly to nanotubes due to electrostatic interactions between deprotonated groups [12]. Since pH is less acidic for the calcium chloride precursor, a stronger adherence of polyacrylate to the nanotubes is observed, more calcium polyacrylate is formed over the surface of nanotubes during gelation, resulting on saturation of the surface and a more densified material. When adapting the method to different cations and salts, the precursor proportions will need to be tuned according to the application specific necessities.

The formation of particles is observed on the surface of the AG-Cu-T aerogel (Fig. 4b), with composition confirmed by EDX (Fig. 4a). Detailed elemental mapping showing the distribution of the particles is available in Figs. S7–S9. The final metal loading of thermal treated aerogels is ~47%wt of Cu for AG-Cu-T and ~9%wt of Ca for AG-Ca-T, calculated from TGA profiles available in Fig. S11 of the supporting information.

Fig. S10 shows the results obtained using UHR SEM (a) of the AG-Ca-T aerogel, where multiple particles adhered to the wall of the nanotubes are observed, these particles have sizes around 10 to 20 nm in diameter. Fig. S10(b) shows the quantification of the EDX analysis in some of these particles finding the presence of calcium and iron. This indicates that nanotubes retain some of the iron, which was used as a catalyst during the synthesis, agreeing with the XPS analysis where Fe remnants can be observed. In Fig. S10(a) it is possible to observe the typical bamboo structure of carbon nanotubes doped with nitrogen. On the other hand, in Fig. S10(c) they observe the samples corresponding to the AG-Cu-T samples corresponding to the sample obtained with copper nitrate, where it is possible to observe that the particles have a size around 20 nm, these particles tend to agglomerate in some places forming clusters on the walls of the nanotubes. EDX analysis was performed in some areas (Fig. S10(d)), identifying the presence of copper and iron, which indicates that the iron remaining from the synthesis was not completely eliminated. In Fig. S10(c) it is possible to observe the typical bamboo structure of carbon nanotubes doped with nitrogen as well as iron particles within the nanotubes, which is typical of carbon nanotubes synthesized by CVD using an iron catalyst.

5. Conclusions

Sodium polyacrylate functionalized carbon nanotube aerogels were prepared on aqueous medium by a simple ionic cross-linking procedure using copper nitrate and calcium chloride as cation sources. The presence of the carboxylate contribution in C1s XPS in the cross-linked calcined materials, suggests the important role that this group has in the thermal stability of the aerogels.

Ion exchange turns water soluble sodium polyacrylate into insoluble calcium or copper polyacrylates by means of the formation of crosslinking coordination bonds between the divalent cation and the carboxylate groups of polyacrylate. The formation of crosslinking produces a gel that acts as a template that guides and reinforces the microstructure, enabling greater degree of order in cross-linked aerogels when in comparison with the prepared without the addition of divalent cations.

In principle the preparation of aerogels using this technique can be done using any divalent cation, with the advantage of the metal oxide particles embedded within the carbon nanotube network. This fact opens the possibility to obtain self-standing carbon nanotube structures with properties and chemical characteristics suitable for different applications in several fields lika catalysis, medicine, energy, and some others.

Declaration of Competing Interest

The authors declare that they have no known competing financial interests or personal relationships that could have appeared to influence the work reported in this paper.

Data Availability

No data was used for the research described in the article.

Acknowledgments

The authors would like to thank: TecNM and CONACYT for their support through TecNM projects 13844.22-P and CONACYT project 319771 and as well as the scholarship 467839, FONCICYT-CONACYT project 299044; M.C. Irma Galindo-Vallarino for the access to the characterization; Dr. Pascual Bartolo Pérez and Ing. Willian Cauich Ruiz for the XPS spectra; LANBIO–CINVESTAV- Mérida for characterization in XRD; M.C. José Bante Guerra for his technical support in obtaining the Raman spectra performed in the Spectroscopy Laboratory, CINVESTAV-IPN; The Materials Characterization Laboratory at The Pennsylvania State University for providing access to the ICDD PDF-4 + 2021 database; and LINAN-IPICYT and Dr. Hector Silva for the characterization in SEM.

Supplementary materials

Supplementary material associated with this article can be found, in the online version, at doi:10.1016/j.cartre.2022.100235.

References

[1] S. Zeng, H. Chen, H. Wang, X. Tong, M. Chen, J. Di, Q. Li, Crosslinked carbon nanotube aerogel films decorated with cobalt oxides for flexible rechargeable Zn-air batteries, Small 13 (29) (2017) 1700518 -.
[2] M. De Marco, F. Markoulidis, R. Menzel, S.M. Bawaked, M. Mokhtar, S.A. Al-Thabaiti, S.N. Basahel, M.S.P. Shaffer, Cross-linked single-walled carbon nanotube aerogel electrodes via reductive coupling chemistry, J. Mater. Chem. A 4 (15) (2016) 5385–5389.
[3] R. Du, et al., Nitrogen-doped carbon nanotube aerogels for high-performance ORR catalysts, Small 11 (32) (2015) 3903–3908 Aug..
[4] Y. Shen, A. Du, X.L. Wu, X.G. Li, J. Shen, B. Zhou, Low-cost carbon nanotube aerogels with varying and controllable density, J. Sol-Gel Sci. Technol. 79 (1) (2016) 76–82.
[5] L. Dong, Q. Yang, C. Xu, Y. Li, D. Yang, F. Hou, H. Yin, F. Kang, Facile preparation of carbon nanotube aerogels with controlled hierarchical microstructures and versatile performance, Carbon 90 (2015) 164–171 2015.
[6] J. Zou, J. Liu†, A.S. Karakoti, A. Kumar, D. Joung, Q. Li, S.I. Khondaker, S. Seal, L. Zhai, Ultralight multiwalled carbon nanotube aerogel, ACS Nano 4 (12) (2010) 7293–7302.
[7] G. Shao, D.A.H. Hanaor, X. Shen, A. Gurlo, Freeze casting: from low-dimensional building blocks to aligned porous structures-a review of novel materials, methods, and applications, Adv. Mater. 32 (17) (2020) 1907176.
[8] F.T. Wall, J.W. Drenan, Gelation of polyacrylic acid by divalent cations, J. Polym. Sci. 7 (1) (1951) 83–88.
[9] V. Linder, B.D. Gates, D. Ryan, B.A. Parviz, G.M. Whitesides, Water-soluble sacrificial layers for surface micromachining, Small 1 (7) (2005) 730–736.
[10] S. Chen, G. Wu, Y. Liu, D. Long, Preparation of poly(acrylic acid) grafted multiwalled carbon nanotubes by a two-step irradiation technique, Macromolecules 39 (1) (2006) 330–334.
[11] A. Liu, I. Honma, M. Ichihara, H. Zhou, Poly(acrylic acid)-wrapped multi-walled carbon nanotubes composite solubilization in water: definitive spectroscopic properties, Nanotechnology 17 (12) (2006) 2845–2849.
[12] J.C. Grunlan, L. Liu, Y.S. Kim, Tunable single-walled carbon nanotube microstructure in the liquid and solid states using poly(acrylic acid, Nano Lett. 6 (5) (2006) 911–915.
[13] X.Y. Chen, C. Chen, Z.J. Zhang, D.H. Xie, J.W. Liu, A general conversion of polyacrylate-metal complexes into porous carbons especially evinced in the case of magnesium polyacrylate, J. Mater. Chem. A 1 (12) (2013) 4017–4025.
[14] F. Rechberger, M. Niederberger, Synthesis of aerogels: from molecular routes to 3-dimensional nanoparticle assembly, Nanoscale Horiz. 2 (1) (2017) 6–30.
[15] A. Du, B. Zhou, J. Shen, J. Gui, Y. Zhong, C. Liu, Z. Zhang, G. Wu, A versatile sol–gel route to monolithic oxidic gels via polyacrylic acid template, New J. Chem. 35 (5) (2011) 1096–1102.
[16] H. Ha, K. Shanmuganathan, C.J. Ellison, Mechanically stable thermally crosslinked poly(acrylic acid)/reduced graphene oxide aerogels, ACS Appl. Mater. Interfaces 7 (11) (2015) 6220–6229.
[17] H. Xiao, J.P. Pender, M.A. Meece-Rayle, J.P. Souza, K.C. Klavetter, H. Ha, J. Lin, A. Heller, C.J. Ellison, C.B. Mullins, Reduced-graphene oxide/poly(acrylic acid) aerogels as a three-dimensional replacement for metal-foil current collectors in lithium-ion batteries, ACS Appl. Mater. Interfaces 9 (27) (2017) 22641–22651.
[18] M. Terrones, R. Kamalakaran, T. Seeger, M. Rühle, Novel nanoscale gas containers: encapsulation of N2 in CNx nanotubes, Chem. Commun. 23 (2000) 2335–2336.
[19] M. Belmonte, S.M. Vega-Díaz, A. Morelos-Gómez, P. Miranzo, M.I. Osendi, M. Terrones, Nitrogen-doped-CNTs/Si3N4nanocomposites with high electrical conductivity, J. Eur. Ceram. Soc. 34 (5) (2014) 1097–1104.
[20] S. Maldonado, S. Morin, K.J. Stevenson, Structure, composition, and chemical reactivity of carbon nanotubes by selective nitrogen doping, Carbon 44 (8) (2006) 1429–1437.
[21] S. Gates-Rector, T. Blanton, The powder diffraction file: a quality materials characterization database, Powder Diffr. 34 (4) (2019) 352–360.
[22] R. Das, S.B.A. Hamid, M.E. Ali, S. Ramakrishna, W. Yongzhi, Carbon nanotubes characterization by X-ray powder diffraction – a review, Curr. Nanosci. 11 (1) (2014) 23–35.
[23] A.C. Ferrari, J. Robertson, Interpretation of Raman spectra of disordered and amorphous carbon, Phys. Rev. B 61 (2000) 14095–14107.
[24] A. Ferrari, Raman spectroscopy of graphene and graphite: disorder, electron-phonon coupling, doping and nonadiabatic effects, Solid State Commun. 143 (2007) 47–57.
[25] A. Sadezky, H. Muckenhuber, H. Grothe, R. Niessner, U. Pöschl, Raman microspectroscopy of soot and related carbona- ceous materials: Spectral analysis and structural information, Carbon 43 (2005) 1731–1742.
[26] J. Filik, Raman spectroscopy: a simple, non-destructive way to characterise diamond and diamond-like materials, Spectrosc. Eur. 17 (2005) 10.
[27] C.C. Zhang, S. Hartlaub, I. Petrovic, B. Yilmaz, Raman spectroscopy characterization of amorphous coke generated in industrial processes, ACS Omega 7 (3) (2022) 2565–2570.
[28] S. Dubinsky, G.S. Grader, G.E. Shter, M.S. Silverstein, Thermal degradation of poly(acrylic acid) containing copper nitrate, Polym. Degrad. Stab. 86 (1) (2004) 171–178.
[29] M. Gopiraman, S.G. Babu, Z. Khatri, W. Kai, Y.A. Kim, M. Endo, R. Karvembu, I.S. Kim, An efficient, reusable copper-oxide/carbon-nanotube catalyst for N-arylation of imidazole, Carbon 62 (2013) 135–148.
[30] T.I.T. Okpalugo, P. Papakonstantinou, H. Murphy, J. McLaughlin, N.M.D. Brown, High resolution XPS characterization of chemical functionalised MWCNTs and SWCNTs, Carbon 43 (1) (2005) 153–161.
[31] H.C. Choi, S.Y. Bae, W.S. Jang, J. Park, H.J. Song, H.J. Shin, H. Jung, J.P. Ahn, Release of N 2 from the carbon nanotubes via high-temperature annealing, J. Phys. Chem. B 109 (5) (2005) 1683–1688.
[32] I.C. McNeill, S.M.T. Sadeghi, Thermal stability and degradation mechanisms of poly(acrylic acid) and its salts: part 3-magnesium and calcium salts, Polym. Degrad. Stab. 30 (3) (1990) 267–282.
[33] V. Datsyuk, M. Kalyva, K. Papagelis, J. Parthenios, D. Tasis, A. Siokou, I. Kallitsis, C. Galiotis, Chemical oxidation of multiwalled carbon nanotubes, Carbon 46 (6) (2008) 833–840.
[34] J.F. Moulder, J. Chastain, in: Handbook of X-ray Photoelectron Spectroscopy: A Reference Book of Standard Spectra For Identification and Interpretation of XPS Data, 40, Physical Electronics Division, Perkin-Elmer Corporation, 1992, pp. 221–261.